Wave patterns from an optical model on Serranilla Island Cays, Colombian Caribbean

Patrones de oleaje a partir de un modelo óptico en la isla Cayos de Serranilla, Caribe Colombiano

DOI: https://doi.org/10.26640/22159045.2022.603 **Received:** 2022-06-16 / **Accepted:** 2022-08-02

Serguei Lonin[1]; Rosana Adames[2]; José Luis Payares[3]; Leonardo Marriaga Rocha[4]

Citation:

Lonin, S.; Adames, R. Payares Varela, J. L.; Marriaga Rocha L. (2022). Wave patterns from an optical model on Serranilla Island Cays, Colombian Caribbean. *Bol. Cient. CIOH;* 41(1): 63-72. Printed ISSN 0120-0542 and Online ISSN 2215-9045. DOI: https://doi.org/10.26640/22159045.2022.603

Abstract

This article presents the methodology used to estimate synthetic bathymetry using Worldview 2 satellite images of the Serranilla Island Cays Colombian Caribbean. The estimate was made for depths of less than five meters. For this, the RGB bands were correlated with in situ bathymetric data, obtained using a single beam echo sounder, with the best correlation found for the Red band. This allowed bathymetric data to be calculated for the shallow areas, thus facilitating the input of data for the implementation of the SWAN spectral wave model in three domains, used to propagate the waves from deep waters to the barrier reef in the vicinity of Serranilla Island Cays , with which the wave patterns for the study area were obtained.

Keywords: Serranilla Island Cays; light propagation model; spectral wave model, reflectance, synthetic bathymetry.

Resumen

En este artículo se presenta la metodología utilizada para estimar batimetría sintética utilizando imágenes satelitales Worldview 2 de isla Cayos de Serranilla, Caribe colombiano. La estimación se realizó para profundidades menores a cinco metros. Para ello, se efectuó una correlación de las bandas RGB con los datos batimétricos in situ, obtenidos con una ecosonda monohaz con mejor correlación para la banda Roja. Lo anterior permitió generar datos batimétricos en las zonas poco profundas, facilitando así, el ingreso de datos para la implementación del modelo espectral de oleaje SWAN en tres dominios, con el fin de propagar el oleaje desde aguas profundas hasta la barrera arrecifal en inmediaciones de la isla Cayos de Serranilla, con lo cual se obtuvo los patrones de oleaje para la zona de estudio.

Palabras clave: *isla Cayos de Serranilla; modelo de propagación de luz; modelo espectral de oleaje, reflectancia, batimetría sintética.*

[1] Orcid: 0000-0001-9561-0554. Escuela Naval de Cadetes "Almirante Padilla. E-mail: slonin@costa.net.co

[2] Orcid 0000-0001-6290-2470. Escuela Naval de Cadetes "Almirante Padilla. E-mail: rpadames@gmail.com

[3] Orcid: 0000-0001-8215-0755. Escuela Naval de Cadetes "Almirante Padilla. E-mail: jlpayares@enap.edu.co

[4] Orcid: 0000-0001-5413-6163. Armada de Colombia. E-mail: leomarriaga@gmail.com

Introduction

In 2000, the Archipelago of San Andrés, Providencia and Santa Catalina was declared as the Seaflower Biosphere Reserve (SBR) by the United Nations Educational, Scientific and Cultural Organization (UNESCO). This reserve covers an approximate area of 180,000 km2 between latitudes 12 and 16° N and between longitudes 78 and 82° W (Colombian Ocean Commission, 2015).

From a hydrodynamic point of view, the SBR area is very active, as it includes a coral barrier reef of great relevance for the Caribbean trophic networks. Currently, the SBR is the site of important research projects involving inter-institutional efforts, such as the recent Seaflower Scientific Expeditions organized by the Colombian Ocean Commission.

Figure 1. Study area. Serranilla Bank.

Serranilla Island Cays corresponds to an atoll with an approximate area of 1 200 km^2 with several island cays, of which Beacon Cay, or Serranilla Cay, will be the focus of this study (CORALINA - INVEMAR, 2012). This bank is bordered by a coral formation located on a volcanic base surrounded by deep water (Correa *et al*., 1996), with an approximate area of 40 x 40 km, and which contributes to the formation of the reef lagoon inside. However, to date, the relationship between wave parameters and the regular and atypical conditions for the formation of the atoll has not been studied in detail, as it requires the use of wave models that are given bathymetric (depth) data of this area of interest (Figure 1).

Bathymetry obtained by the use of passive remote sensing has become an important method for obtaining water depth information because of its wide coverage, the possibility to rapid update it, and its low cost. The traditional ship- or boat-based bathymetric survey method is accurate, but it is not applicable in areas that cannot be accessed by these vessels. Satellite altimetry is often used to produce bathymetry estimates, but can be very inaccurate in shallow water (Lee *et al*., 2010).

Lidar sounding can be used to measure water depth in areas that boats cannot reach, such as regions around islands and reefs, but it is expensive to use and covers narrow measurement ranges (Zhang, Ma and Zhang, 2020).

In the coastal zone, thanks to the fact that sunlight can reach the bottom, bathymetry is a fundamental parameter that can be determined using the proportion of light that is reflected, due to the water or bottom albedo, and reaches a passive optical remote sensor such as those used in most satellites (Abasolo, J., 2016). Additionally, at the coast, the seabed is coupled to hydrodynamic processes generated mainly by wave dynamics.

In order to validate the readings obtained from satellite images of the Serranilla Island Cays, we proposed to determine the characteristics of the bottom reflectance in shallow waters, which make it possible to infer bathymetric data where it has not been possible to obtain echo sounder data. The wave climate and its propagation were obtained using spectral models of high spatial resolution.

Methodology

Synthetic Bathymetry

Seabed reflectance characterization was performed from Worldview 2 satellite images (Table 1) in order to generate an estimated synthetic bathymetry of the study area.

Table 1. Characteristics of the WorldView 2 images used in the study.

Name	ATCORCorrected_13NOV05160503-M2AS-054958618020_01_p001_083
Spectral resolution	7 (R, G, B, N, NDWI, NDVI, ICEDEX)
Spatial resolution	2 m
Radiometric resolution	32 Bits
Temporal resolution	1.1 día
Reference system	UTM 17 N
Datum	WGS84

The images were provided by the Caribbean Oceanographic and Hydrographic Research Center (CIOH) and the Agustín Codazzi Geographic Institute (IGAC), and were previously treated with atmospheric correction using the Empirical Linear Model (ELM) (Baugh and Groeneveld 2008, Hadjimitsis *et al*. 2010, and Schott 1997) and the ATCOR model (Richter and Schläpfer 2005), which have a high capacity to remove atmospheric effects.

For the ELM correction, Ariza and Roa (2015) used spectral signatures collected in the field with an HR4000 spectroradiometer to measure coral formations, vegetation (palms), submerged sands and dry sands, achieving a correlation higher than 90% between in situ data and satellite image values for the RGB (Red Green Blue) bands.

To identify the band of the visible spectrum that best matched the bathymetric data, ArcGIS 10.5 was used to extract the reflectance of each of the RGB bands and make the respective comparison, which made it possible to identify the one that best matched the in situ bathymetry data for the first 5 meters of depth.

Wave patterns

Two third-generation spectral wave models, WAVEWATCH III™ (WW-III) and Simulating Waves Nearshore (SWAN), were used to establish wave patterns. For this purpose, the deep-water wave climate was established from a virtual buoy (the closest computational node of the WW-III model); then, the wave was propagated in three domains (nested grids in Figure 2) using the SWAN model with the following wave climate boundary conditions: 1) extended domain of 55 x 46 km with a spatial resolution of 200 m, 2) intermediate domain of 15 x 11 km with a spatial resolution of 50 m, and 3) study area domain of 1554 x 1400 m with a spatial resolution of 5 m.

The first two domains used bathymetric data obtained by CIOH using echo sounders up to 2017. To model the conditions in the vicinity of the barrier reef, it was necessary to previously generate bathymetry in shallow areas, so synthetic bathymetry was used as an input for wave simulation in the third calculation domain.

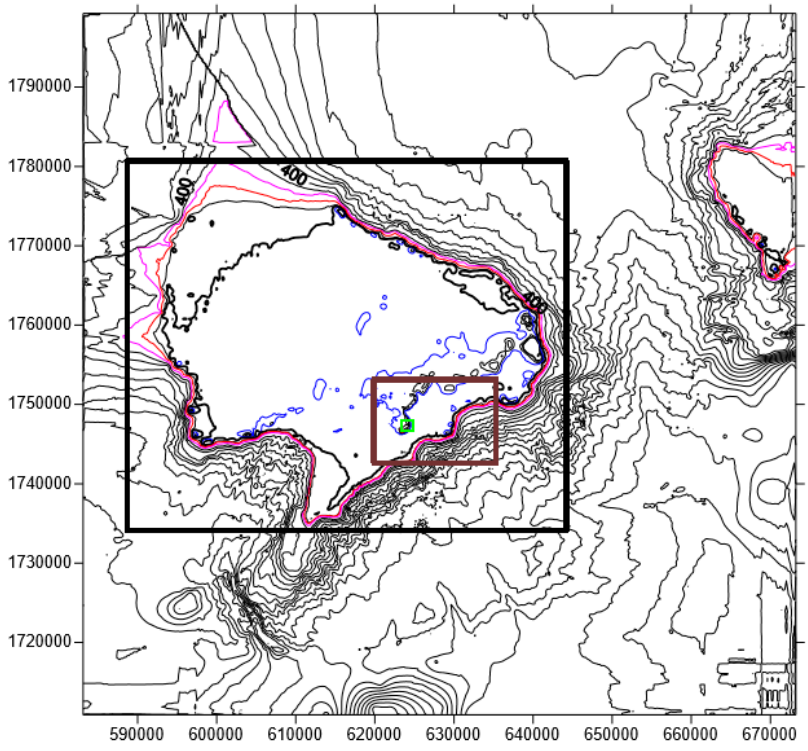

Figure. 2. Selection of the three calculation domains: extended domain (black), intermediate domain (brown), study area domain (green).

Results and Discussion

Optical properties

The reflectance information obtained through the processing of Worldview 2 satellite images and the bathymetric data provided by the CIOH for the study area was verified, through which it was found that good estimates of depths less than 5 m were obtained using the reflectance of the red band (R(630-690 nm)), while the blue (B(450-510 nm)) and green (G(510-580 nm)) bands did not show a good correlation; this can be seen in Figure 3.

Depending on the transparency of the water, the short waves of the visible range of the light spectrum reach the depth of the photic layer, while the near infrared (NIR) and red (R) bands are absorbed within a few centimeters and the first meters, respectively, of the water column. This explains why the R band is the best associated with the depths of the first 3 m.

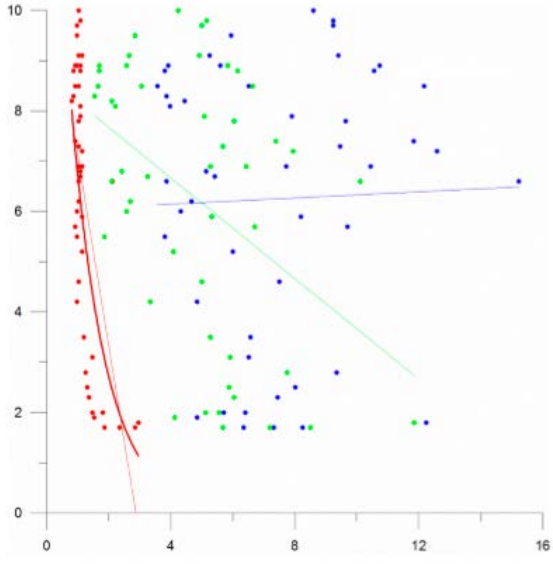

Figure 3. Correspondence of RGB reflectance (vertical axis) versus depth in meters (horizontal axis). RGB = f(h). The colors correspond to the respective bands of visible light: R (red), G (green) and B (blue).

Figure 4 shows the coverage of reflectance data generated from the satellite images for the study area, associated with depths between 0 and 5 meters.

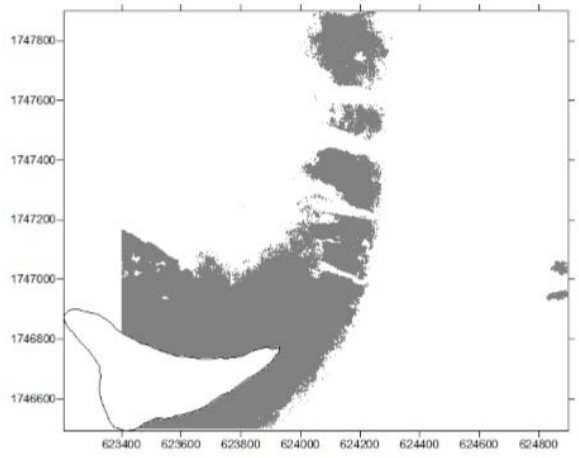

Figure 4. Coverage of the pixels of the image corresponding to depths of less than 5 m. Study area domain from Figure 1.

When analyzing the correlation between the depth found by the R-band reflectance and that measured with the echo sounder (Figure 5), it can be seen that there are two types of curves, apparently due to the bottom substrate (sand vs. coral). This leads to the need to study the dependence of reflectance on bottom type.

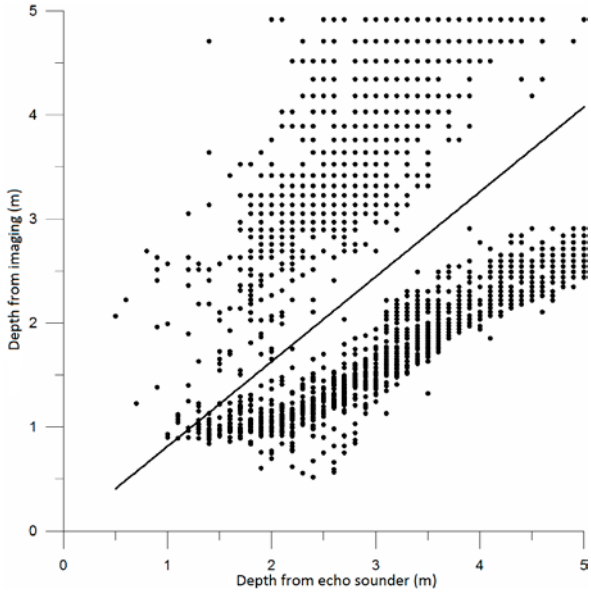

Figure. 5. Correlation between the depth calculated from R-band reflectance and that measured directly by echo sounder.

Figure 5 shows the correlation with the R-band for these two bottom types. The curve fitting corresponds to the following expressions:

Sandy bottom:

$$\ln(\rho R) = -0.963567 \ln(H) + 2.39366 \quad \textbf{(1)}$$

Coral bottom:

$$\ln(\rho R) = -0.89205 \ln(H) + 1.31259 \quad \textbf{(2)}$$

In equations (1) and (2), rR is the reflectance in the Red band (0-255) and H represents the depth in meters. In both cases, the fit is logarithmic. Coral reflects with lower intensity compared to sands for the same depth.

The light reflectance for the two bottom types is shown in Figure 6. The higher values correspond to the white calcareous sands on the seabed and the lower ones to the coral surfaces. Finally, in Figure 7, the synthetic seabed (depth in m) in the vicinity of the barrier reef was composed by combining echo sounder bathymetry and equations (1) and (2).

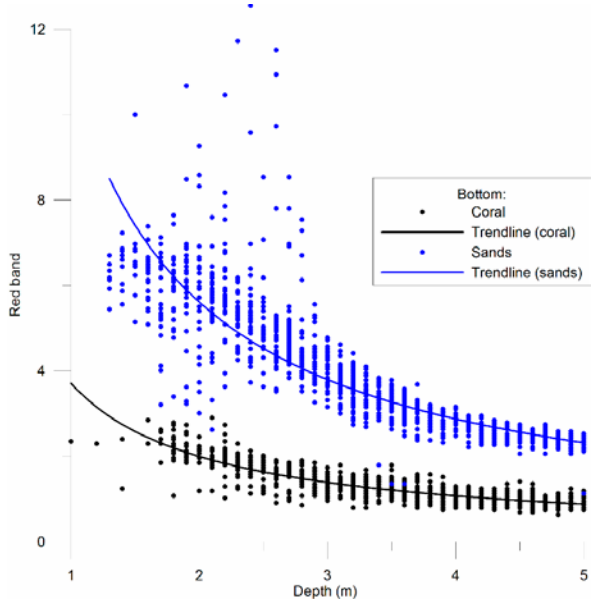

Figure 6. Depth-dependence of the R-band data for the two bottom types.

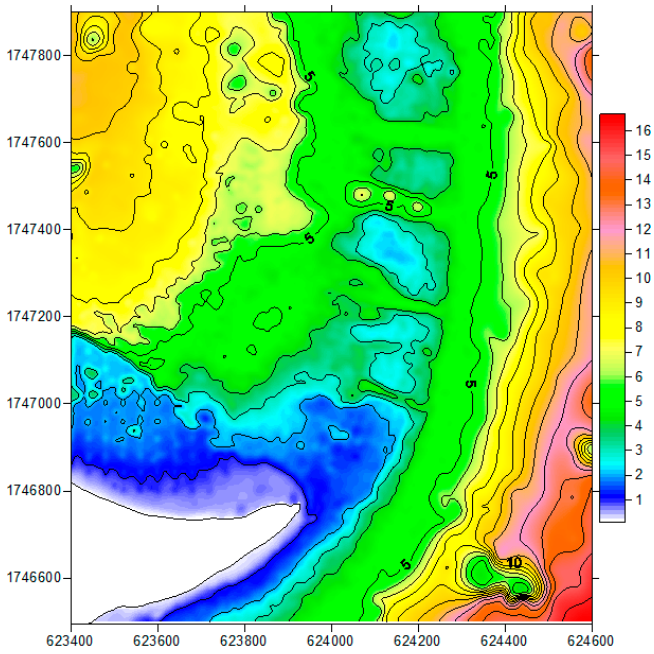

Figure 7. Synthetic seabed (depth in m), calculated for nested domain No. 3, based on the WorldView 2 image and echo sounding data (CIOH).

Wave patterns

The behavior of the waves, coming from one of the nodes closest to the cay (corresponding to the study area of the spectral model) and using pseudo reanalysis data from the WAVEWATCH III model, is shown in Figure 8. The statistics include the significant wave height (Hs, Figure 8a), the peak period (Tp, Figure 8b) and the wave direction (Figure 8c) for the last 20 years. The regime wave (multiannual) has a significant height of 1.69 m, a peak period of 7.3 s and a direction of 93° E. As for the predominant swell (Figure 8d), the direction of greatest probability is East (E) followed by East-Southeast (ESE).

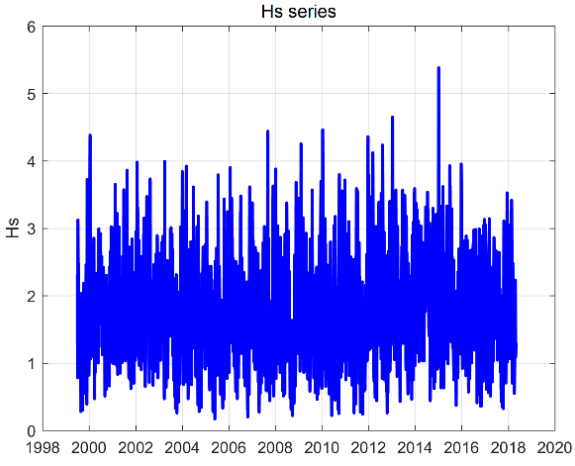

(a)

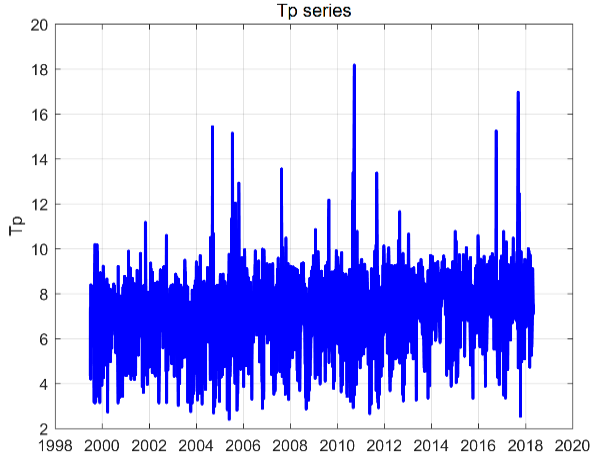

(b)

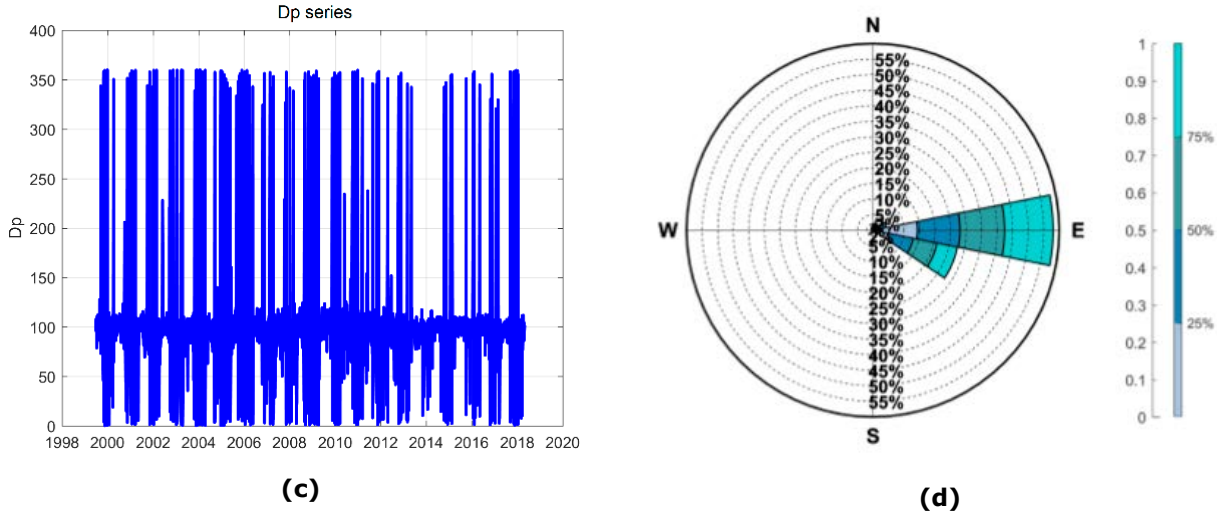

Figure 8. Time series for: **(a)** Significant height (m), **(b)** Peak period (s) and **(c)** Nautical direction (degrees) in deep water at a nearby node in WW-III; and **(d)** Swell rose (significant height in m).

Figures 9-11 illustrate the outputs of the SWAN model for the extended, intermediate and study area domains respectively, considering typical swell conditions.

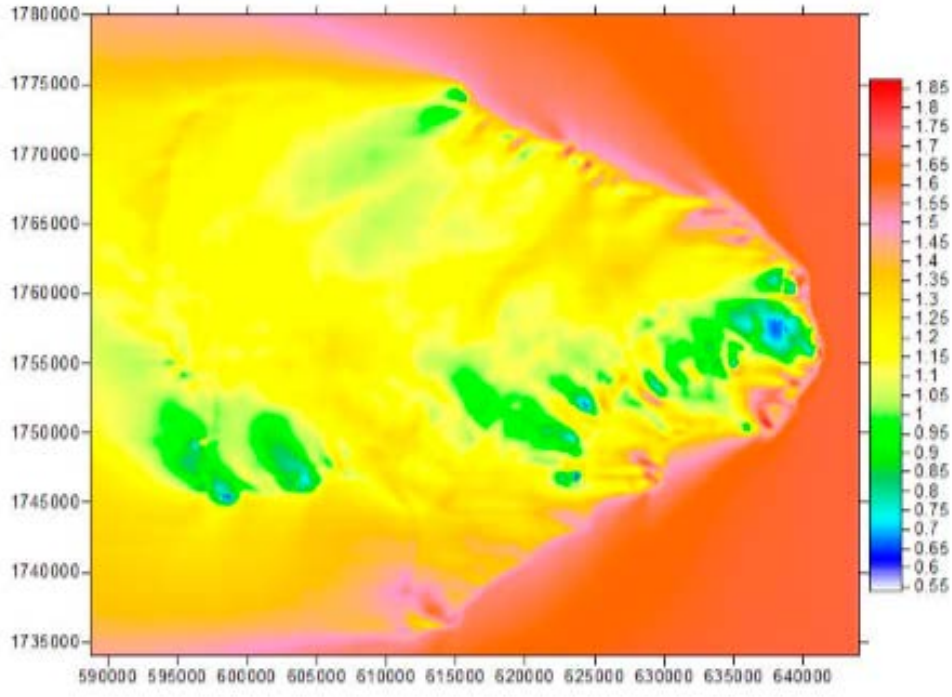

Figure 9. Wave propagation (significant height in meters) for the extended domain under the dominant weather conditions, analyzed with data from the WW-III model. Outputs of the SWAN model.

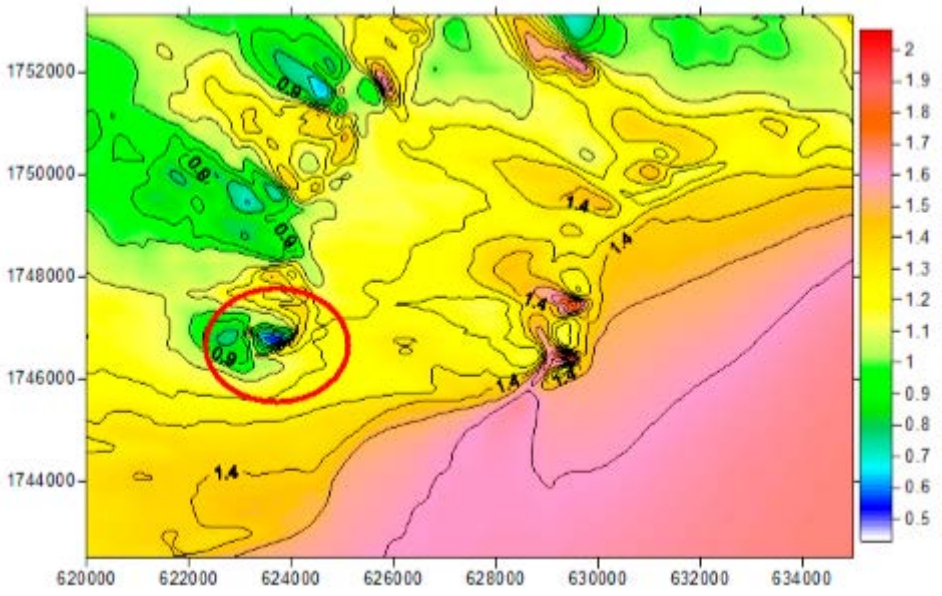

Figure 10. Wave propagation (significant height in meters) for the intermediate domain under the dominant weather conditions, analyzed with data from the WW-III model. Outputs of the SWAN model. The red circle highlights Beacon Cay.

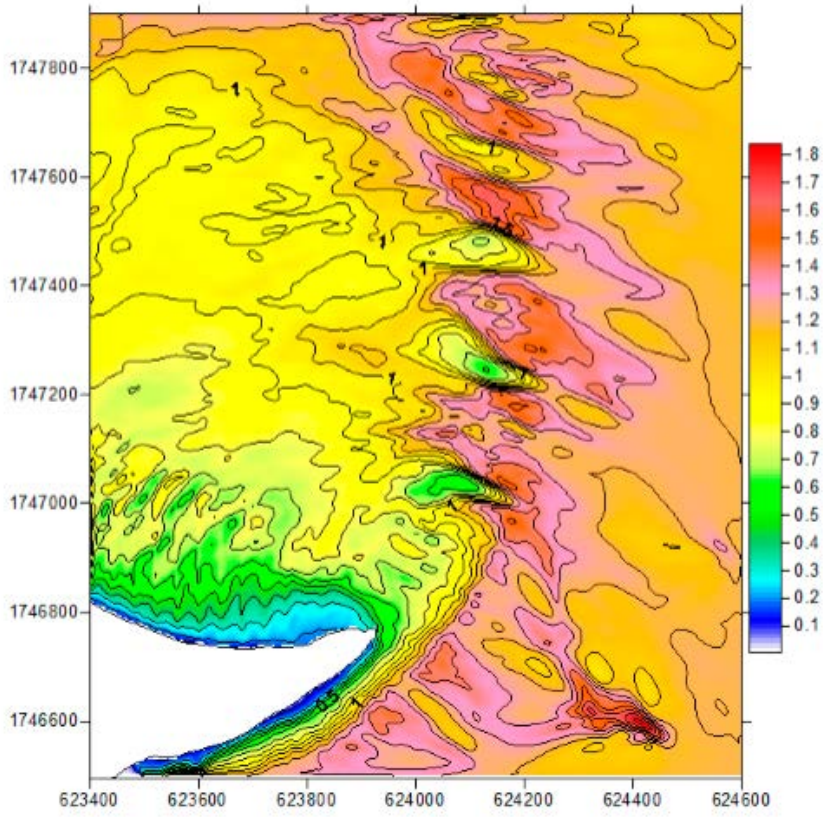

Figure 11. Wave propagation (significant height in meters) for the study area domain under the dominant weather conditions, analyzed with data from the WW-III model. Nested grid from the SWAN model.

According to Figure 12, the wave direction in the vicinity of the Cay suffers the effect of refraction due to the relief of the seabed. The calculation corresponds to a wave height of 1.69 m, peak period of 7.3 s and deep water direction of 93° (E).

It is observed that, inside the atoll, to the north of the island, the incident wave has a direction of 10-20° (it arrives practically perpendicular to the coast); while, in the southern part, the angle is 130-140° (SE). However, it should be clarified that the direction and length of the waves underwent a significant change across the barrier reef and the waves shown in Figure 11 (generally within the atoll, on the north coast) have decreased as they cross the reef.

Therefore, it is important to consider the "single" angle of the mean wave energy direction in deep water (93°), found based on the wave climate and corresponding to the favorable conditions for the past formation of the barrier reef with its present orientation.

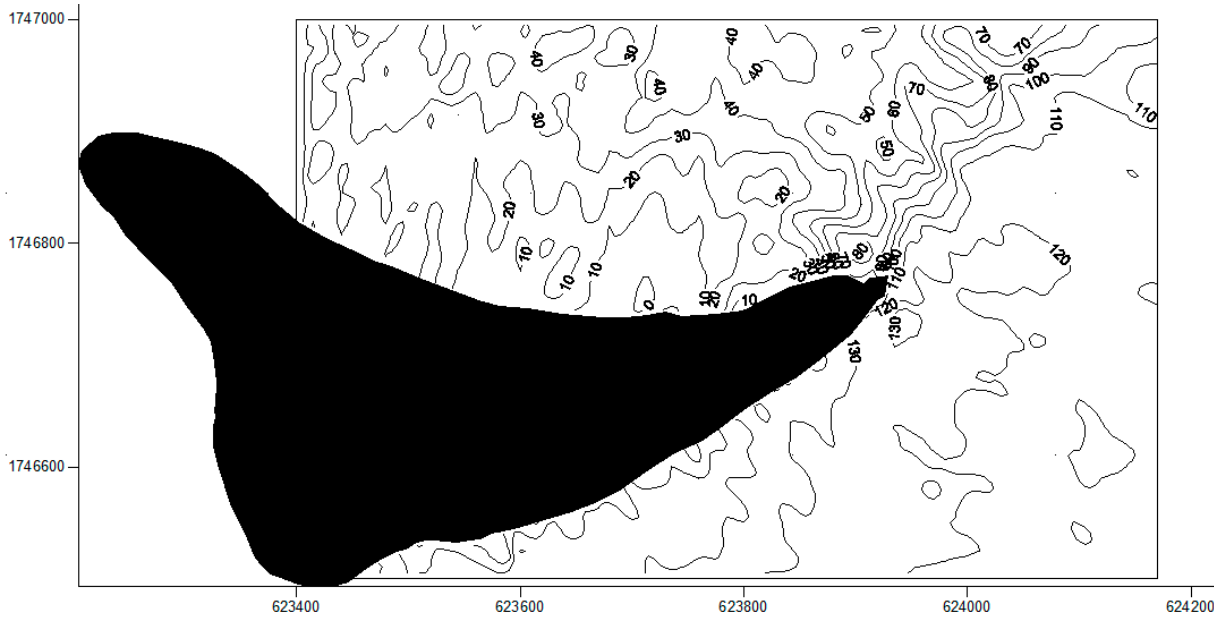

Figure 12. Mean propagation direction (in degrees) of waves based on the principal pattern in deep waters.

Zambrano and Andrade (2011) described the local waves at Beacon Cay using the OLAS module and performing spectral analysis of the waves from in situ data obtained from pressure sensors anchored near the beach at a depth between 1.5 and 2.0 m for periods of 6 hours. To do so, they classified the beaches of the cay by sectors, concluding that the predominant characteristic waves in the northern sector come from the Northeast-east (NEE) with a probability of occurrence of 37.8%.

For the south beach, the characteristic wave direction is from the East-Southeast (ESE) with a probability of occurrence of 32.8%, and for the west beach, the predominant direction is from the Northwest (NW) with a probability of occurrence of 1.1% (Tejada, 2002). Considering that the study analyzed the local waves on the cay, these wave directions most likely correspond to the refraction of the predominant swell in the study area, which in fact comes from the east.

Conclusions

From the bottom reflectance obtained by processing the Wordview 2 images of Serranilla Island Cays, the R band is the one that is best associated with the depths of the first 3 m. By correlating the bottom reflectance with the in situ data, logarithmic profiles were obtained for two

curves, apparently associated with the different bottom substrate (sands and coral). The wave climate was obtained for 20 years (until 2018) obtaining a significant height of 1.69 m, a peak period of 7.3 s and a direction of 93° E. In the vicinity of Beacon Cay, the effect of refraction by the bottom could be evidenced and corroborate the direction of the waves with respect to the coral reef.

Acknowledgments

This research was carried out thanks to the support of the Colombian Navy, the Colombian Ocean Commission, the General Maritime Directorate, the Center for Oceanographic and Hydrographic Research of the Caribbean, and the Agustin Codazzi Geographic Institute, in the framework of the 2017 Seaflower Scientific Expedition, Serranilla Island Cays.

Bibliography

Abasolo, J. (2016). *Implementación de algoritmos para la monitorización de calidad de aguas y de espacios costeros mediante la utilización de imágenes de teledetección satelital de muy alta resolución*. Tesis doctoral cibernética y telecomunicación. Universidad de Las Palmas de Gran Canaria, Departamento de Señales y Comunicaciones.

Ariza, A.; Roa, O. (2015). *Informe técnico corrección atmosférica de imágenes Worldview-2 mediante el modelo empírico lineal*. Contrato No. 041 GINRED4/2015, suscrito entre el Ministerio de Defensa-Dirección General Marítima-Intendencia Regional Dimar y el Instituto Geográfico "Agustín Codazzi" (IGAC).

Baugh, W.; Groeneveld, D. (2008). Empirical proof of the empirical line. *International Journal of Remote Sensing*. Vol. 29, Issue 3, pp. 665-672. https://doi.org/10.1080/01431160701352162

Comisión Colombiana del Océano. (2015). *Aportes al conocimiento de la Reserva de Biósfera Seaflower.* CCO. Bogotá D.C. 108 pp.

Corporación para el Desarrollo Sostenible del Archipiélago de San Andrés, Providencia y Santa Catalina-Instituto de Investigaciones Marinas y Costeras "José Benito Vives de Andréis". (2012). Gómez-López, D. I.; Segura-Quintero, C.; Sierra-Correa, P. C.; Garay-Tinoco, J. (Eds). *Atlas de la Reserva de Biósfera Seaflower.* Coralina-Invemar. Serie de Publicaciones Especiales de Invemar N°. 28. Santa Marta, Colombia, 180 pp.

Correa, M.; Valderrama, J.; Montes, S. (1996). *Archipiélagos del Caribe Colombiano.* Cali: Banco de Occidente.

Hadjimitsis, D.; Papadavid, G.; Agapoiu, A.; Themistocleus, K.; Hadjimitsis, M.; Retalis, A.; Michaelides, S.; Chysoilaskis, N.; Toulios, L.; Clayton, C. (2010). Atmospheric corection for satellite remotely sensed data intended for agricultural application: impacto on vegetation índices. *Natural HAzards and Earth System Sciences*. Vol. 10:89-95. https://doi.org/10.5194/nhess-10-89-2010

Lee, Z.; Hu, C.; Casey, B.; Shang, S.; Dierssen, H.; Arnone, R. (2010). Global Shallow-Water Bathymetry From Satellite Ocean Color Data. *AGU Advance Earth and Space Science.* Vol. 91, Issue 46, pp. 429-430. https://doi.org/10.1029/2010EO460002

Richter, R.; Schläpfer, D. (2005). *Atmospheric/ topographic correction for satellite imagery.* DLR report DLR-IB, 565-601. Recuperado de http://www.rese.ch/pdf/ atcor3_manual.pdf

Schott, J. (1997). Remote sensing. The image chain approach. *Geological Magazine,* 136(6): 697-711.

Tejada, C. (2002). Desarrollo de un módulo informático para el manejo de datos de oleaje visual para las aguas jurisdiccionales colombianas. *Bol. Cient. CCCP*, 9:88-98. https://doi.org/10.26640/01213423.9.59_66

Zambrano, J.; Andrade, C. (2011). Cambios en la línea de costa del Cayo Serranilla entre 1944 y 2009, Archipiélago de San Andrés, Colombia. *Bol. Cient. CIOH,* 29:87-103. https://doi.org/10.26640/22159045.231

Zhang, X.; Ma, Y.; Zhang, J. (2020). Shallow Water Bathymetry Based on Inherent Optical Properties Using High Spatial Resolution Multispectral Imagery. *Remote Sens. 12*(18), 3027. https://doi.org/10.3390/rs12183027